Coaxial-Fed Dual-Layer SIW Horn Antenna With Improved E-Plane Radiation Pattern

Mahbubeh Esmaeili, Jens Bornemann
Department of Electrical and Computer Engineering, University of Victoria, Victoria, BC, V8W 3P6, Canada
mesmaei@uvic.ca

***Abstract*—A novel technique is introduced to improve the directivity of the E-plane pattern of substrate integrated waveguide (SIW) horn antennas. While the H-plane directivity of a SIW horn antenna is good, SIW horns have a wide E-plane radiation pattern due to the thin substrates of SIW circuits. Increasing the substrate height to improve the E-plane half power beam width (HPBW) makes it difficult to fabricate vias by current technologies. As a solution, two identical SIW horns are stacked to increase the E-plane profile of the antenna. A hole with diameter of 0.35 mm is incorporated in the substrate to accommodate a coaxial feeding port. The designed antenna has a 10-dB bandwidth of 5.37 percent and a gain of 10.33 dB at 21.5 GHz. The robustness of the design approach is validated by measurements which are in good agreement with simulations.**

Keywords—Substrate integrated waveguide (SIW); horn antenna; directivity; E-plane pattern; HPBW; coaxial feed.

I. Introduction

Substrate integrated waveguide (SIW) components have been widely investigated due to their advantages of low profile and low conductive losses which make them appropriate for high frequency applications and planar circuitry. In addition, they have more power handling capability in comparison to conventional microstrip circuits.

SIW antennas are widely reported in the literature for different applications such as a microfluidic resonator antenna for chemical sensor applications [1], and an all-textile substrate integrated waveguide antenna consisting of a cavity feed structure and a circular ring-slot for wireless body area network applications [2].

SIW horn antennas are the most commonly used antennas when a high gain end-fire radiation pattern as well as low fabrication cost and weight are required. Much effort has been put into introducing novel SIW horn antennas with improved characteristics. In [3], higher gain of a SIW horn antenna is obtained by extending the substrate and loading it with a dielectric waveguide at the aperture. A combination of a dielectric loaded aperture and printed transition in front of the aperture is reported in [4] to enhance the antenna gain. In order to increase the impedance bandwidth, a SIW horn antenna is loaded with an air-via perforated dielectric in [5] which results in 10-dB bandwidth of 40 percent. Another technique is introduced in [6] to increase the antenna bandwidth based on ridged substrate integrated waveguide with a large conducting ground. A method is proposed in [7] to overcome the difficulties of SIW horn antennas below 30 GHz with a substrate thinner than $\lambda_0/10$. A SIW horn antenna phase correction technique is introduced in [8] to increase the antenna gain without deteriorating its bandwidth. All the reported SIW horn antennas in the literature consist of a single horn or a planar array of several horns [9].

Despite all above mentioned progress in SIW horn antenna characteristics, their E-plane directivity, due to the small height of the substrate, remains a challenge. Due to difficulties of plating a via hole in a very thick substrate, it is not possible to directly increase the E-plane profile of a SIW horn in order to increase its E-plane directivity. Therefore, in this paper, for the first time, we introduce a new configuration of a SIW horn antenna to improve its E-plane half power beam width (HPBW). The proposed design is based on increasing the E-plane profile of the antenna by stacking two separate SIW horns (Fig. 1a) and feeding both at a single coaxial port through a hole inside the substrate of the horns.

II. Antenna Design

The design process starts with designing a single SIW horn antenna at a frequency of 21.5 GHz. The design rules for SIW horn antennas follow the principles for conventional H-plane horns and, therefore, the same strategies to improve their performance can be used for a single SIW horn antenna. Maximum directivity and minimum phase error at the antenna aperture is obtained when [10]

$$w_1 \approx \sqrt{3\lambda\rho} \tag{1}$$

where w_1 is the aperture width, λ is the wavelength inside the horn antenna, and ρ is the length of the horn which is related to the flare angle φ by (Fig. 1b)

$$\rho = \frac{w_1}{2}\cot(\varphi) \tag{2}$$

To ensure a TE_{10} mono-mode excitation in the feeding waveguide section of the horn, the width a is chosen as [10]

$$\frac{\lambda_0}{2\sqrt{\varepsilon_r}} \le a \le \frac{\lambda_0}{\sqrt{\varepsilon_r}} \tag{3}$$

where λ_0 is the wavelength in free space, and the substrate height, h, is smaller than a.

Three parallel plates are located in front of the radiating aperture, as shown in Fig. 1b, to improve the antenna's bandwidth by smoothing impedance changes between the

This work was supported by the TELUS Research Grant in Wireless Communications

antenna aperture and free space. Each transition is studied as a parallel-plate resonator separated from other transitions by a distance *s*. The length of the transition can be calculated by [4]

$$\frac{2\pi L}{\lambda_0} + \beta_{pp} L = (2n+1)\pi \ , \quad n \in Z \tag{4}$$

and

$$\beta_{pp} = \frac{2\pi\sqrt{\varepsilon_{rpp}}}{\lambda_0} \tag{5}$$

β_{pp} is the propagation constant of the parallel plate waveguides. The effective permittivity ε_{rpp} can be calculated by the quasi-static approximation and figures presented in [11].

The resonance frequency of a single parallel-plate resonator is obtained by [12]

$$f_{r1} = \frac{c}{2L_{eq}\sqrt{\varepsilon_r}} \tag{6}$$

where L_{eq} is an equivalent length that is larger than L due to fringing fields. The parameter L_{eq} can be estimated by [13]

$$L_{eq} = L(1 + 0.7\frac{h}{L}) \tag{7}$$

and h is the antenna's height which equals the substrate thickness.

When there are two blocks of parallel-plate resonators, separated by distance *s*, two resonant frequencies, f_{r2-}, lower than f_{r1}, and f_{r2+}, greater than f_{r1}, are generated. In coupled resonator theory, a coupling factor k_2 is defined to calculate $f_{r2\pm}$

$$f_{r2\pm} = \frac{f_{r1}}{\sqrt{1 \mp k_2}} \tag{8}$$

More details about calculating k_2 vs. *s* is presented in [12]. The number of transmission zeros in the antennas' reflection coefficient equals the number of transitions, and detailed design guidelines are presented in [12]. Three parallel-plate transitions are used in our SIW horn design to achieve a 1.15 GHz bandwidth at 21.5 GHz. Two parallel plates are resonating at the same frequency to provide a better return loss (more than 15 dB) in the antenna's band.

A 50-Ohm coaxial port is used as a feed which goes through the substrate by means of a plated via hole. The location of the coaxial port in the waveguide section of the horn is optimized to minimize the reflection coefficient at the feed point.

In the second step, a second horn antenna is placed on the top of the first one. To obtain the best results, both horn antennas are identical, and parallel plates are located only on the outer layers of the antenna structure. Fig. 1 shows the details of the final antenna design. All dimensions are presented in Table I. The antenna flare angle for best radiation properties is obtained as φ=18.8°.

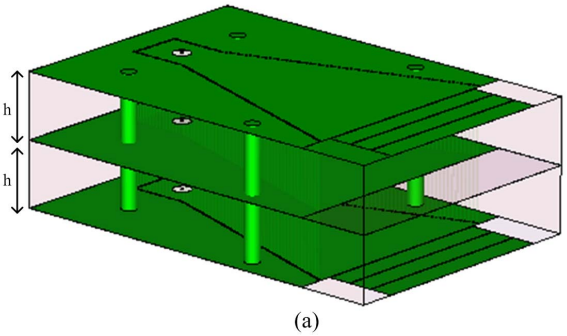

(a)

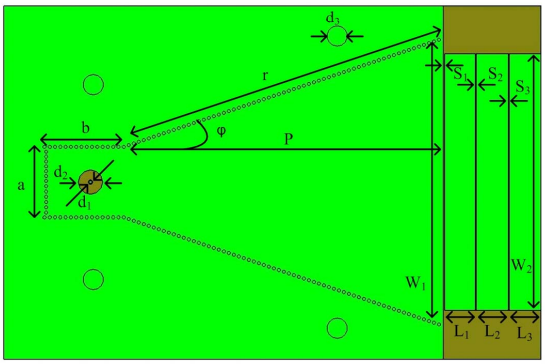

(b)

Fig. 1. 3D view of the designed antenna presenting different layers (a), and the antenna's top view (b).

TABLE I. ANTENNA PARAMETERS (MILLIMETERS)

L_1	3.75	r	40.95
L_2	3.90	d_1	0.35
L_3	3.90	d_2	3.00
W	35.06	d_3	2.50
a	8.68	S_1	0.15
b	9.75	S_2	0.15
W_2	31.64	S_3	0.15
h	2.54	P	38.76

III. ANTENNA FABRICATION AND MEASUREMENTS

For fabrication purposes, four non-plated holes are inserted into the substrate of each single antenna, and plastic screws are used to tighten the antennas after fabrication. The top and bottom views of the antenna prototype are depicted in Fig. 2. Rogers RT5880LZ with dielectric constant of 1.96 and loss tangent of 0.0019 is used as the SIW substrate. The metallization thickness is 17.5 µm, and the diameter of all side wall vias is 0.4 mm. A K-band coaxial connector with a 0.3 mm diameter pin is connected to the antenna for measuring purposes. The inside of the feeding via hole is filled with conductive paste to lengthen the coaxial pin through the entire height of the dual-layer antenna.

Simulated and measured return loss performances are presented in Fig. 3. The measured 10-dB impedance bandwidth

is 5.37 % at the center frequency of 21.5 GHz which is in good agreement with simulations. The slight downward frequency shift in the measured results is attributed to the fact that after fabrication, the metallization thickness increases due to the copper flow to metallize the vias. According to (7) and (6), this decreases the resonant frequency.

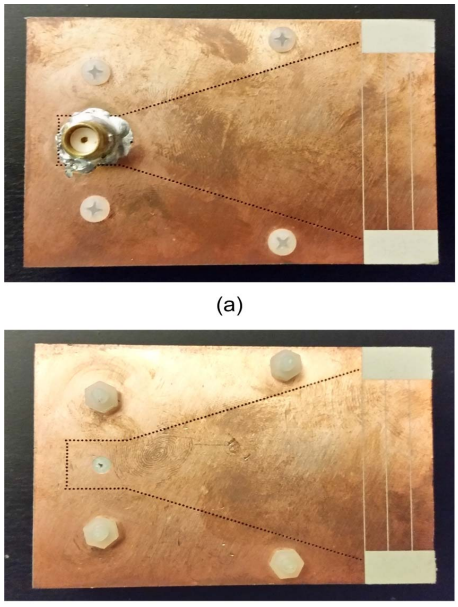

(a)

(b)

Fig. 2. Prototyped antenna; bottom view (a), top view (b).

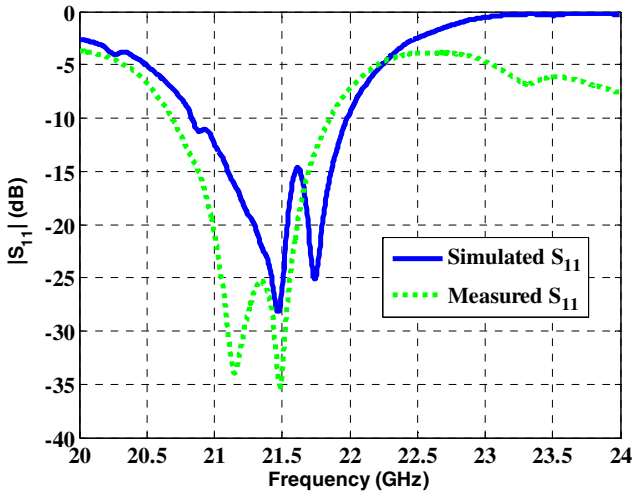

Fig. 3. Comparison between measured and simulated reflection coefficients.

The measured and simulated H-plane co-pol and cross-pol patters are shown in Fig. 4. The simulated H-plane half power beam width (HPBW) of the antenna is 27.6° which is well confirmed by measurement. The isolation between co-pol and cross-pole is measured as 24.12 dB in the main beam direction. The about 10 dB higher measured cross-pol levels are attributed to some metal parts in the mount of the SIW antenna that could not entirely be covered by absorber material.

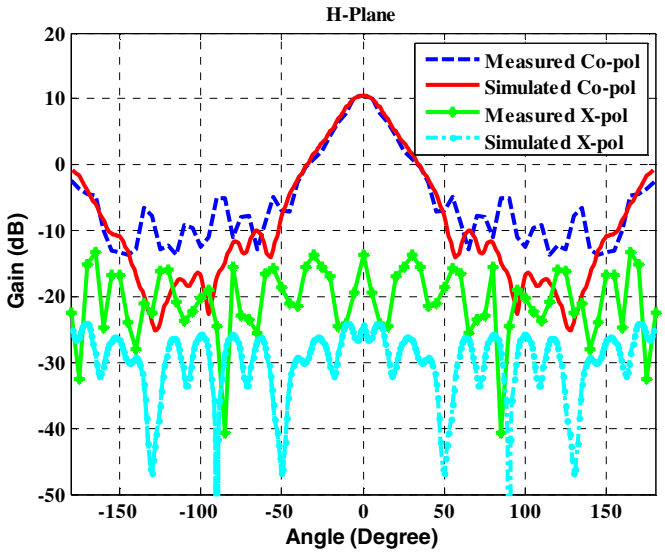

Fig. 4. Measured and simulated H-plane co-pol and cross-pol radiation patterns at 21.5 GHz

Fig. 5 presents the measured and simulated E-plane co-pol and cross-pol patterns. The measured E-plane HPBW of 75° is in good agreement with the simulated value of 73.8°. A 25 dB isolation between E-plane co-pol and cross-pol levels is measured in the main beam direction. The asymmetries in the patterns are attributed to the coaxial feed and attached cable which also influence the cross-pol performance.

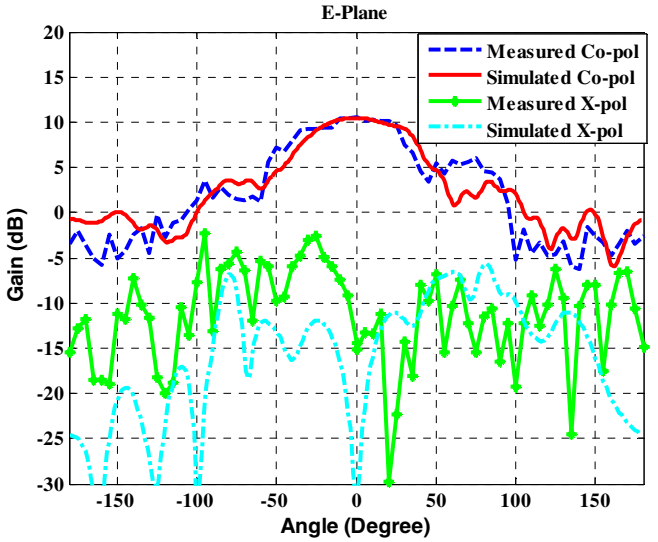

Fig. 5. E-plane co-pol and cross-pol radiation patterns; simulation vs. measurement at 21.50 GHz

The measured and simulated antenna gains are depicted in Fig. 6. The measured gain varies between 10.33 dB at 21.50 GHz and 7.90 dB at 22 GHz and is in good agreement with simulations. The gain degradation toward the upper band limit (beyond 21.8 GHz) is attributed to the slight increase in cable losses which have been assumed to be constant over the frequency range of interest.

Table II compares the E-plane HPBW of this work with those reported in the literature for a single SIW horn. It is obvious that the dual-layer SIW horn proposed here presents an improvement towards narrower E-plane beam width.

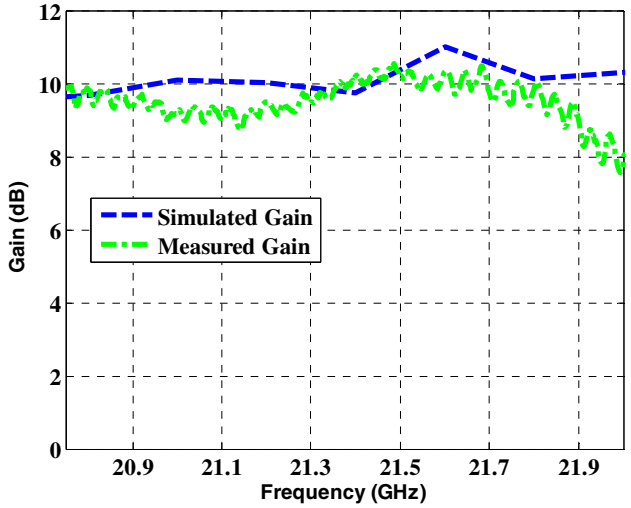

Fig. 6. Simulated and measured antenna gain.

TABLE II. E-PLANE HPBW COMPARISON

	This Work	Ref. [8]	Ref. [7]	Ref. [3]
E-plane HPBW	75°	90°	120°	120°

IV. CONCLUSION

A novel coaxial-fed dual-layer SIW horn antenna is presented to increase the directivity of a conventional SIW horn. The designed antenna consists of two separate and vertically stacked SIW horns. The final design has a thicker E-plane profile which results in an obvious improvement of the E-plane half power beam width. Measurements on a prototype are in good agreement with simulations and validate the design approach.

REFERENCES

[1] Y. Seo, M. U. Memon, and S. Lim, "Microfluidic eigth-mode substrate-integrated waveguide antenna for compact ethanolchemical sensor application," *IEEE Trans. Antennas Propag*., vol. 64, no. 7, pp. 3218-3222, July 2016.

[2] Y. Hong, J. Tak, and J. Choi "An all-textile SIW cavity-backed circular ring-slot antenna for WBAN application," *IEEE Antennas Wireless Propag. Lett.*, vol. 15, pp. 1995-1999, 2016.

[3] H. Wang, D. G. Fang, B. Zhang, and W. Q. Chen, "Dielectric loaded substrate integrated waveguide (SIW) H-plane horn antennas," *IEEE Trans. Antennas Propag*., vol. 58, no. 3, pp. 640-647, Mar. 2010.

[4] Y. Tang, Z. Wang, L. Xia, and P. Chen, "A novel high gain K-band H-plane SIW horn antenna using dielectric loading," in *Proc. Asia-Pacific Microw. Conf*., Sendai, Japan, Nov. 2014, pp. 372-374.

[5] Y. Cai, Z. P. Qian, Y.S. Zhang, J. Jin, and W.Q. Cao, "Bandwidth enhancement of SIW horn antenna loaded with air-via perforated dielectric slab," *IEEE Antennas Wireless Propag. Lett*., vol. 13, pp. 571-574, 2014.

[6] Y. Zhao, Z. Shen, and W. Wu, "Wideband and low-profile H-plane SIW horn antenna mounting on a large conducting plane," *IEEE Trans. Antennas Propag*., vol. 62, no. 11, pp. 5895-5900, Nov. 2014.

[7] M. Esquius-Morote, B. Fuchs, J. F. Zurcher, and J. R. Mosig, "Novel thin and compact H-plane SIW horn antenna," *IEEE Trans. Antennas Propag*., vol. 61, no. 6, pp. 2911-2920, June 2013.

[8] L. Wang, M. Esquius-Morote, H. Qi, X. Yin, and J. R. Mosig, "Phase corrected H-plane horn antenna in gap SIW technology," *IEEE Trans. Antennas Propag*., vol. 65, no. 1, pp. 347-353, Jan. 2017.

[9] M. Esquius-Morote, J. F. Zurcher, J. R. Mosig, and , B. Fuchs "Low-profile SIW horn antenna array with interconnection to MMICs," in *Proc. German Microw. Conf*., Aachen, Germany, Mar. 2014, pp. 1-3.

[10] C. A. Balanis, *Antenna Theory: Analysis and Design*, 3rd ed. NewYork, NY, USA: Wiley, 2005.

[11] P. Benedek, and P. Silvester, "Capacitance of parallel rectangular plates separated by a dielectric sheet," *IEEE Trans. Microw. Theory Tech*., vol. 20, no. 8, pp. 504-510, Aug. 1972.

[12] M. Esquius-Morote, B. Fuchs, J. F. Zurcher, and J. R. Mosig, "A printed transition for matching improvement of SIW horn antennas," *IEEE Trans. Antennas Propag*., vol. 61, no. 4, pp. 1923-1930, Apr. 2013.

[13] K. Y. Yazdandoost and D. C. Gharpure, "Simple formula for calculation of the resonant frequency of a rectangular microstrip antenna,"in *Proc. IEEE Int. Symp. Spread Spectrum Techniques and Applications*, vol. 2, Sun City, South Africa, Sep. 1988, pp.604-605.